

See discussions, stats, and author profiles for this publication at: <https://www.researchgate.net/publication/257248666>

Studies on the interactions of bioactive quinone avarone and its methylamino derivatives with calf thymus DNA

ARTICLE *in* INTERNATIONAL JOURNAL OF BIOLOGICAL MACROMOLECULES · SEPTEMBER 2013

Impact Factor: 2.86 · DOI: 10.1016/j.ijbiomac.2013.09.013 · Source: PubMed

CITATIONS

3

READS

36

6 AUTHORS, INCLUDING:



Miroslava T Vujcic

University of Belgrade

41 PUBLICATIONS 365 CITATIONS

SEE PROFILE



Irena Novakovic

University of Belgrade

27 PUBLICATIONS 161 CITATIONS

SEE PROFILE



Daniela Djikanovic

University of Belgrade

20 PUBLICATIONS 154 CITATIONS

SEE PROFILE



Studies on the interactions of bioactive quinone avarone and its methylamino derivatives with calf thymus DNA

Miroslava T. Vujčić^{a,*}, Srđan Tufegdžić^a, Irena Novaković^a, Daniela Djikanović^b,
Miroslav J. Gašić^c, Dušan Sladić^d

^a Institute of Chemistry, Technology and Metallurgy, Department of Chemistry, University of Belgrade, Njegoševa 12, 11000 Belgrade, Serbia

^b Institute for Multidisciplinary Research, Kneza Višeslava 1, 11000 Belgrade, Serbia

^c Serbian Academy of Sciences and Arts, Knez Mihailova 35, Belgrade, Serbia

^d Faculty of Chemistry, University of Belgrade, Studentskitrg 16, Belgrade, Serbia

ARTICLE INFO

Article history:

Received 15 March 2013

Received in revised form

13 September 2013

Accepted 17 September 2013

Available online 28 September 2013

Keywords:

Avarol

Avarone

3'-(Methylamino)avarone

4'-(Methylamino)avarone

Calf thymus DNA

Fluorescence measurements

ABSTRACT

The interactions of avarone, a quinone from the marine sponge *Dysidea avara*, and the methylamino derivatives of avarone (**2**), 3'-(methylamino)avarone (**3**) and 4'-(methylamino)avarone (**4**) with calf thymus DNA (CT-DNA) were studied. Agarose gel electrophoretic analysis showed that binding of the quinones quenched fluorescence of ethidium bromide (EB). The extent of fluorescence quenching of intercalator EB by competitive displacement from EB–CT-DNA system and of groove binder Hoechst 33258 (H) from H–CT-DNA system with the quinones was analyzed by fluorescence spectroscopy. The obtained results demonstrated that the quinones reduced binding of both the intercalator EB and the minor groove binder H, indicating possible degradation of DNA. The substituent on the quinone moiety determined the extent of DNA damaging effect of the quinone, which was the most extensive with 3'-(methylamino)avarone and the least extensive with its regioisomer 4'-(methylamino)avarone. The results were confirmed by the observed hyperchromic effects in UV–visible spectra measured after interactions of the derivatives with CT-DNA.

© 2013 Elsevier B.V. All rights reserved.

1. Introduction

Deoxyribonucleic acid (DNA), which contains the genetic instructions for the development and functioning of living organisms is an obvious focus of attraction for many researchers. DNA is the target molecule of many drugs, especially antitumor agents. A large number of low molecular weight molecules, synthetic and natural products or their derivatives recognize DNA and interact with DNA double helix structures in different non-covalent modes: intercalation, groove binding, external electrostatic effects and three-way junction binding [1,2]. Intercalation occurs by inserting a molecule between stacked base pairs thereby distorting the DNA backbone conformation. Minor groove binders cause little distortion of the DNA backbone. When DNA-reactive molecules form complexes with double-stranded helices it results in marked changes in absorbance and fluorescence properties compared to their spectral characteristics when free in solution [3,4]. On the

other side, DNA damage may be a result of covalent modification of nucleobases and/or strand cleavage by a variety of oxidizing or alkylating/aryllating species such as quinones [5]. Many sesquiterpenoid quinones from marine origin have attracted much interest in recent years due to their interesting pharmacological properties including antitumor, anti-inflammatory, antipsoriasis, and antiviral activity [6]. Avarol is a sesquiterpenoid hydroquinone from the marine sponge *Dysidea avara* and avarone is the corresponding quinone. The antitumor activity of the quinone/hydroquinone couple avarone/avarol (compounds **1** and **2**, Fig. 1) [7] is well known. Biological activity of derivatives of the quinone avarone such as antibacterial action, brine shrimp toxicity and cytotoxicity to tumor cells have been demonstrated recently [8]. Among these compounds methylamino derivatives proved to be of special interest due to their strong activity and difference in effects of regioisomers. Therefore, the methylamino derivatives of avarone (**2**) 3'-(methylamino)avarone (**3**) and 4'-(methylamino)avarone (**4**) were synthesized following the scheme represented in Fig. 1. The study of the binding of these compounds to calf thymus DNA (CT-DNA) would provide an opportunity to understand the selectivity and efficiency of DNA damage by quinone compounds. The damage to CT-DNA by **2**, **3** and **4** was analyzed by agarose gel electrophoresis. The different structural features on the quinone ring may result in different DNA binding modes. The possibilities of the compounds

* Corresponding author at: Institute of Chemistry, Technology and Metallurgy, Department of Chemistry, Njegoševa 12, POB 815, 11001 Belgrade, Serbia. Tel.: +381 11 2636 061; fax: +381 11 2636 061.

E-mail addresses: mvujcic@chem.bg.ac.rs, miravujcic61@gmail.com (M.T. Vujčić).

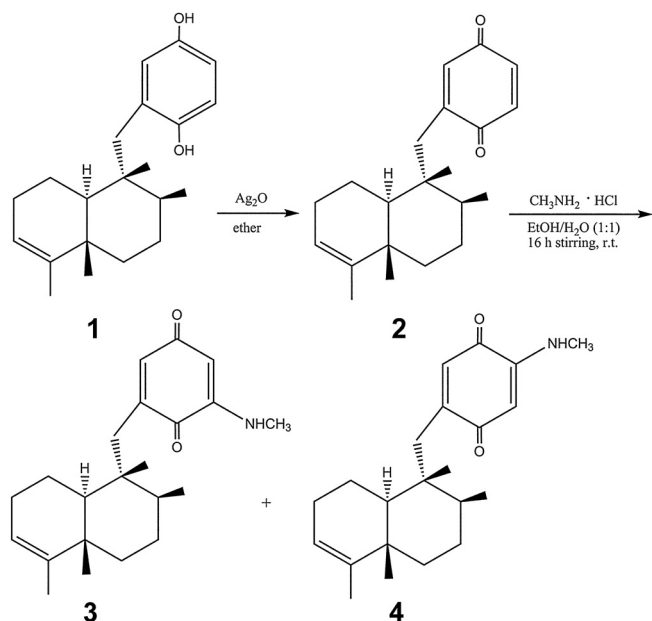


Fig. 1. Scheme for synthesis of avarone and methyl(amino) derivatives; **1** – avarol, **2** – avarone, **3** – 3'-(methylamino)avarone, **4** – 4'-(methylamino)avarone.

to interfere with intercalator of DNA ethidium bromide and with groove binder Hoechst 33258 were investigated by fluorescence spectrometry. In addition, the interaction with CT-DNA was investigated by UV–vis spectroscopy.

2. Experimental

2.1. Chemicals

Avarol (**1**) was isolated from the sponge *Dysidea avara*, collected in the Bay of Kotor (Montenegro) as previously described [9]. Avarone was obtained from its corresponding hydroquinone avarol by oxidation with silver oxide [10]. 3'-(Methylamino)avarone and 4'-(methylamino)avarone were prepared from avarone and methylaminehydrochloride [11]. The supplementary information to this paper provides ^1H NMR, ^{13}C NMR and mass spectroscopic data of the compounds (Figs. S1–S6). ^1H and ^{13}C NMR spectra were recorded at 200 MHz (Oxford NMR YH) in deuterated methanol and mass spectra were recorded on Mass Spectrometer 6210 Time-of-Flight LC–MS system (Agilent Technologies). Calf thymus DNA (lyophilized, highly polymerized) was obtained from Serva, Heidelberg. Agarose was purchased from Amersham Pharmacia-Biotech, Inc.

Supplementary material related to this article can be found, in the online version, at <http://dx.doi.org/10.1016/j.ijbiomac.2013.09.013>.

2.2. Preparation of reagents

All buffer solutions for reactions of the quinones with DNA were prepared in deionized water and filtered through 0.2 μm filters (Nalgene, USA). Stock solutions (10 mg/mL) of **2**, **3** and **4** were prepared by dissolving the substance in ethanol. Lyophilized calf thymus DNA (CT-DNA) was dissolved in 20 mM Tris-HCl pH 7.5/20 mM NaCl overnight at 4 °C. DNA concentration was adjusted with buffer to 3 mg/mL of CT-DNA (9.24 mM, calculated per phosphate). This stock solution was stored at 4 °C and was stable for several days. A solution of CT-DNA in water gave a ratio of UV absorbance at 260 and 280 nm, A_{260}/A_{280} of 1.89–2.01, indicating that DNA was sufficiently free of protein. The concentration of DNA

was determined from the UV absorbance at 260 nm. One optical unit corresponds to 50 $\mu\text{g mL}^{-1}$ of double stranded DNA (based on the known molar absorption coefficient value of 6600 $\text{M}^{-1}\text{cm}^{-1}$) [12].

2.3. Electrophoretic analysis

An incubation mixture (1 mL) consisted of 5 μL of stock solution of CT-DNA and 5 μL of the ethanolic quinone solution in 40 mM bicarbonate solution (pH 8.4). Reaction mixtures were incubated at 37 °C for 90 min with vortexing from time to time. To 10 μL of the reaction mixtures were added 5 μL of the loading buffer (0.25% bromophenol blue, 0.25% xylene cyanol FF and 30% glycerol in water). The samples were subjected to electrophoresis on 0.8% agarose gel prepared in TAE buffer pH 8.24 (40 mM Tris-acetate, 1 mM EDTA, pH 8.0). The electrophoresis was performed at a constant voltage (80 V) for about 1.5 h (until bromophenol blue had passed through 75% of the gel). After electrophoresis, the gel was stained for 30 min by soaking it in an aqueous ethidium bromide solution (0.5 $\mu\text{g mL}^{-1}$). The stained gel was illuminated under a UV transilluminator Vilber-Lourmat (France) at 312 nm and photographed with a Panasonic DMC-LZ5 Lumix Digital Camera.

2.4. Fluorescence measurements

The competitive interactions of quinones and fluorescence probe ethidium bromide with CT-DNA have been studied by measuring the change of fluorescence intensity of each DNA–quinone solution after addition of ethidium bromide. Reaction mixtures containing 92.4 μM of CT-DNA (calculated per phosphate) and different concentrations of the quinone in 1 mL of 40 mM bicarbonate solution (pH 8.4) were incubated for 90 min with occasional vortexing. 1 μL of 1% ethidium solution (25 μM final concentration) was added to each solution, and the incubation was prolonged for the next 30 min and the mixture was analyzed by fluorescence measurement. The control was DNA–ethidium bromide solution. The solutions of quinones did not have fluorescence under applied conditions. Fluorescence spectra were collected using a Fluorolog-3 spectrofluorometer (Jobin Yvon Horiba, Paris, France) equipped with a 450 W xenon lamp and a photomultiplier tube. The slits on the excitation and emission beams were fixed at 4 and 2 nm respectively. The emission spectrum of the solvent was subtracted. All measurements were performed at controlled temperature of 25 °C by means of a Peltier element, by excitation at 500 nm (optimum wavelength) in the range of 520 nm to 700 nm.

The competitive interactions of quinones and fluorescence probe Hoechst 33258 (28 μM at final concentration) with CT-DNA were performed as described above for ethidium bromide. The control was CT-DNA–Hoechst 33258 solution. Fluorescence spectra were collected using a Thermo Scientific Lumina Fluorescence spectrometer (Finland) equipped with a 150 W Xenon lamp. The slits on the excitation and emission beams were fixed at 5 nm. All measurements were performed by excitation at 350 nm in the range of 390–600 nm. The details are given in figure legends.

2.5. UV–visible measurement

For an UV–vis measurement, to DNA solution (10 μL of CT-DNA stock solution) was added a small volume of a concentrated solution of quinone (final concentration 300 μM) and the volume was adjusted up 1 mL with 40 mM bicarbonate buffer pH 8.4. Reaction mixtures were incubated at 37 °C during 2 h with occasional vortexing. Spectra of CT-DNA of the same concentrations were also recorded. UV–vis spectra were recorded in a UV Cintra 40 UV/Visible spectrometer operating from 200 to 800 nm in 1.0 cm quartz cells. UV–vis spectroscopic study was not performed with

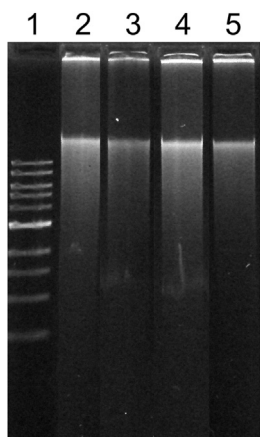


Fig. 2. Agarose gel electrophoresis of CT-DNA after treatment with 3 mM **(2)** (lane 3), **(3)** (lane 4) and **(4)** (lane 5); lane 1: marker DNA; lane 2: control CT-DNA (without quinones).

2, because it was not sufficiently soluble in aqueous solutions used for the study.

2.6. Results processing

Primary spectra of all spectrophotometric measurements were imported into Microcal ORIGIN v8.0 and were processed by this software package.

3. Results and discussion

3.1. Electrophoretic study

Interaction of quinones with DNA has been the subject of extensive studies because quinone groups are present in important chemotherapeutic drugs. It was shown that the quinone/hydroquinone moieties in avarol and derivatives are essential for their cytotoxic activities [6]. In order to assess the damage to DNA resulting from interactions with avarone and its methylamino derivatives, agarose gel electrophoresis has been performed with CT-DNA after treatment with **2**, **3** and **4**. The qualitative visualization of the intensity difference among electrophoretic lanes is shown in Fig. 2. Electrophoretic pattern shows that binding of the quinones quenched the fluorescence of ethidium bromide (EB) in all samples as compared to the control with CT-DNA which had not been treated with the compounds (Fig. 2, lane 2). This capability of compounds to interfere with the intercalation of ethidium bromide in molecule of CT-DNA was the most pronounced with the original compound **2** (Fig. 2, lane 3), followed by **4** (Fig. 2, lane 5), and **3** (Fig. 2, lane 4). The result suggests that the position of the methylamino substituent on the quinone ring is important for the interaction with DNA. It is interesting to note that regioisomer **4** which was more effective in EB fluorescence quenching was the most active compound to melanoma Fem-X cells [8], and also was more efficient than **3** in covalent modifications of proteins [13].

3.2. Fluorescence studies

For the study of the binding mode between the quinone compounds and CT-DNA, the relative binding characteristics such as quenching constant were determined by fluorescence spectroscopy. It is known that the fluorescence of a fluorophore can be quenched by interacting with some quenching molecules through excited-state reactions, molecular rearrangements, energy transfer, ground-state complex formation and collisional quenching

process [14]. Quenching data are usually presented as plots of F_0/F versus $[Q]$ based on the Stern–Volmer equation [15]:

$$\frac{F_0}{F} = 1 + K_{SV} [Q] \quad (1)$$

where F_0 and F are the fluorescence intensities in the absence and presence of a quencher, respectively; K_{SV} is a quenching constant and $[Q]$ is the concentration of quencher. A plot of F_0/F versus $[Q]$ yields an intercept of one on the y-axis and a slope equal to K_{SV} , and K_{SV}^{-1} is the quencher concentration at which $F_0/F = 2$ or 50% of the intensity.

In the work quinones **2–4** had no obvious fluorescence under applied experimental conditions and ethidium bromide (EB) was chosen as a probe to investigate the interactions of avarone and the derivatives with CT-DNA. It is known that EB interacts with CT-DNA in the intercalation mode with a strong binding affinity [16,17]. The extent of fluorescence quenching of EB by competitive displacement from DNA is a measure of the strength of interaction between the second molecule and DNA [18]. The emission spectra of EB bound to CT-DNA in the absence and presence of **2**, **3** and **4** are given in Fig. 3A, B and C, respectively. Binding of ethidium bromide to the CT-DNA was followed by excitation at 500 nm with maximum in fluorescence at 596 nm. The fluorescence intensity of the band at 596 nm of the EB–CT-DNA system decreased remarkably with the increasing concentration of the quinone compounds. The maximal decrease of fluorescence intensity of EB–CT-DNA by avarone (**2**) (Fig. 3A) was 47%, by 3'-(methylamino)avarone (**3**) 52% (Fig. 3B) and by 4'-(methylamino)avarone (**4**) 24% (Fig. 3C). Results showed that the competition of **4** with EB in binding to DNA was less efficient than of **2** and **3**.

The obtained fluorescence quenching data were analyzed according to the Stern–Volmer equation:

$$\frac{I_0}{I} = 1 + K r \quad (2)$$

where I_0 and I represent the fluorescence intensities of EB–CT-DNA in absence and presence of the quinones, respectively, K is a Stern–Volmer quenching constant dependent on the ratio of the bound concentration of ethidium bromide to the bound concentration of DNA; r is the ratio of the concentration of quinone to that of CT-DNA. The fluorescence quenching curves of EB bound to DNA by **2**, **3** and **4** are shown in Fig. 3D, E and F, respectively. The quenching plots illustrate that the quenching of EB–CT-DNA by all quinone compounds presents the Stern–Volmer plot based on Eq. (2), which was applied to determine K by linear regression of a plot of I_0/I against r . The plots displayed a good linear relationship with the correlation coefficients 0.99 ± 0.05 , 0.95 ± 0.09 and 1.00 ± 0.02 for the investigated concentration ranges of **2** (Fig. 4A), **3** (Fig. 4B) and **4** (Fig. 4C), respectively. From the slopes of the plots in Fig. 3D and 3E, the quenching constants of EB–CT-DNA system by **2** and **3** were calculated as $K = 0.123 \pm 0.012$ and 0.147 ± 0.022 , respectively. The best fitting was obtained for quenching fluorescence by **4** (Fig. 3E), with K value of 0.036 ± 0.001 .

The results indicate a good agreement of the interactions between quinones and EB–CT-DNA with the model based on Eq. (1) which means that static quenching process occurred due to fluorophore–quencher complex formation [19], i.e. EB–CT-DNA–quinone complex. The K values for **2**, **3** and **4** suggest that the effects of avarone and 3'-(methylamino) derivative are stronger than those of 4'-(methylamino) derivative. Some deviation of linearity of the plots (Fig. 3D, E) indicates that the observed quenching is due to the quinone induced displacement of ethidium from the EB–CT-DNA system by the non-intercalation mode. A covalent modification of the nucleobases by quinones, or effects of radical species [20], might also be responsible for inhibition of EB to intercalate.

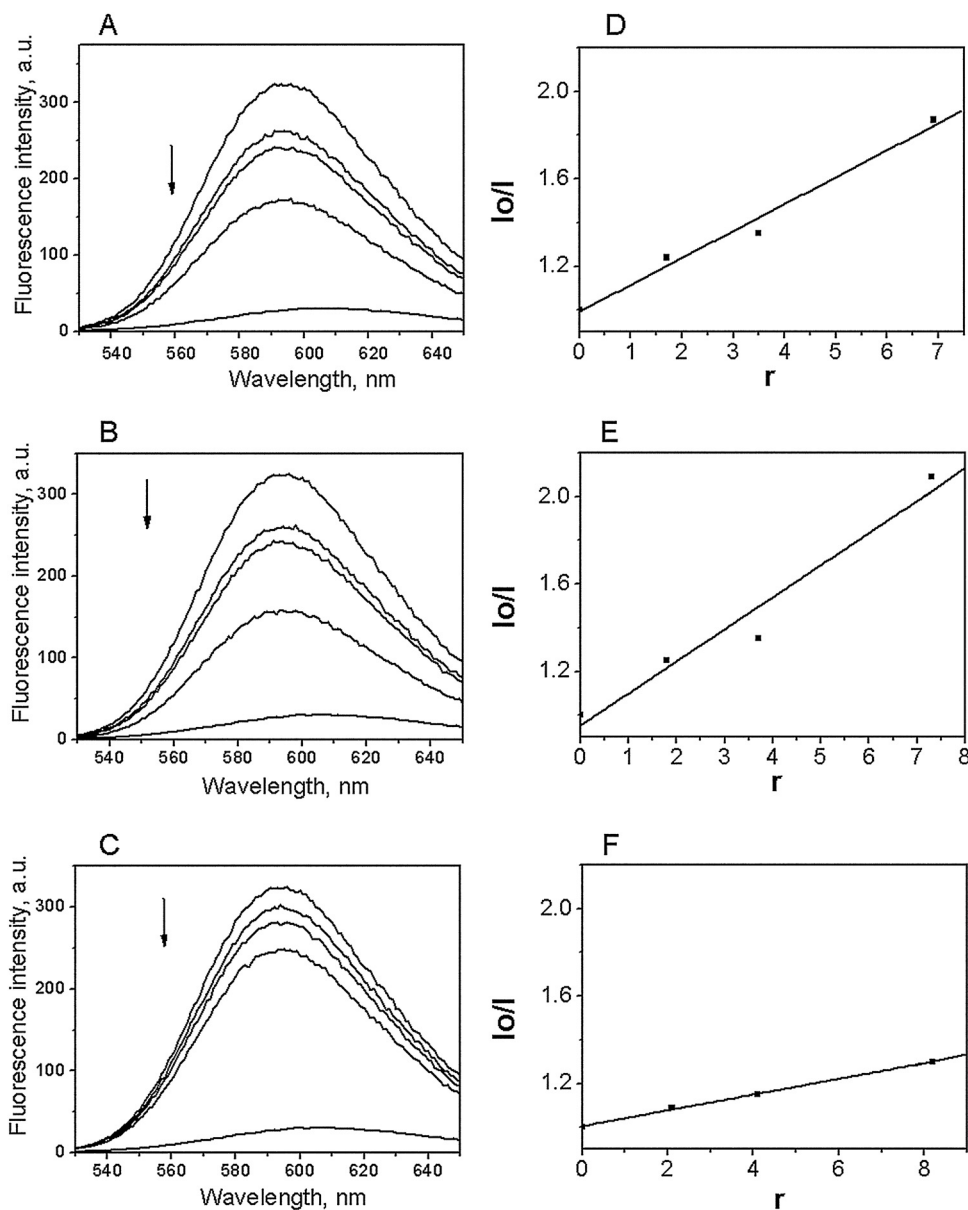


Fig. 3. Quinone interference of intercalative binding of ethidium bromide (EB) with CT-DNA. Left panels: emission spectra ($\lambda_{\text{ex}} = 500$ nm) of EB alone (25 μM , bottom line), EB bound to CT-DNA (92 μM , top line) and quenching of EB-CT-DNA system by quinones **2** (A), **3** (B) and **4** (C) at concentrations of 160 μM , 320 μM and 640 μM (curves from top to bottom). The arrow shows that fluorescence intensity decreased with increasing concentration of the quinone. Right panels: fluorescence quenching curves of EB bound to DNA at $\lambda_{\text{max}} = 595$ nm by **2** (D), **3** (E) and **4** (F); $r = [\text{quinone}]/[\text{CT-DNA}]$.

To provide additional insight into the interactions between the macromolecule and ligands, the experiments with the minor groove binder Hoechst 33258 [21] were performed. Hoechst 33258 (H) binds strongly and selectively with high affinity to double-stranded B-DNA structure and like other minor groove binders, it recognizes at least four AT base pairs. It binds by combination of hydrogen bonding, van der Waals contacts with the walls of the minor groove, and electrostatic interactions between its cationic structure and the DNA [22]. Fig. 4 shows the characteristic changes in fluorescence emission spectra of Hoechst 33258 after binding to DNA i.e. significant increase in the fluorescence intensity of H-CT-DNA compared to free Hoechst. As shown in Fig. 4, the addition of the quinone compound to CT-DNA caused appreciable reduction in the fluorescence intensity of H-CT-DNA complex in a concentration dependent way. The quenching of H-CT-DNA was the most efficient with derivative **3**, Fig. 4B (this derivative quenched fluorescence completely at the maximal applied concentration

640 μM), followed by avarone (**2**) (Fig. 4A) and derivative **4** (Fig. 4C). These results were consistent with quenching curves shown in Fig. 4D–F that were applied to determine K by linear regression of a plot of I_0/I against r . The quenching plots demonstrated the quenching of H bound to CT-DNA by all the compounds are in agreement with the linear Stern–Volmer Eq. (2) with the correlation coefficients 0.81 ± 0.14 , 1.08 ± 0.47 and 1.04 ± 0.02 for the investigated concentration ranges of **2** (Fig. 4D), **3** (Fig. 4E) and **4** (Fig. 4F), respectively. The corresponding quenching constants of H-CT-DNA system by **2**, **3** and **4** were calculated as $K = 0.60 \pm 0.05$, 1.12 ± 0.32 and 0.07 ± 0.01 , respectively. Deviation from linearity might be a consequence of other processes such as base modification and/or nicks formation. As in experiments with ethidium bromide, the derivative **3** was the most efficient, followed by **2**, and **4** was the least efficient agent.

The fact that the quinones inhibit binding of both the intercalator ethidium bromide and the minor groove binder Hoechst 33258

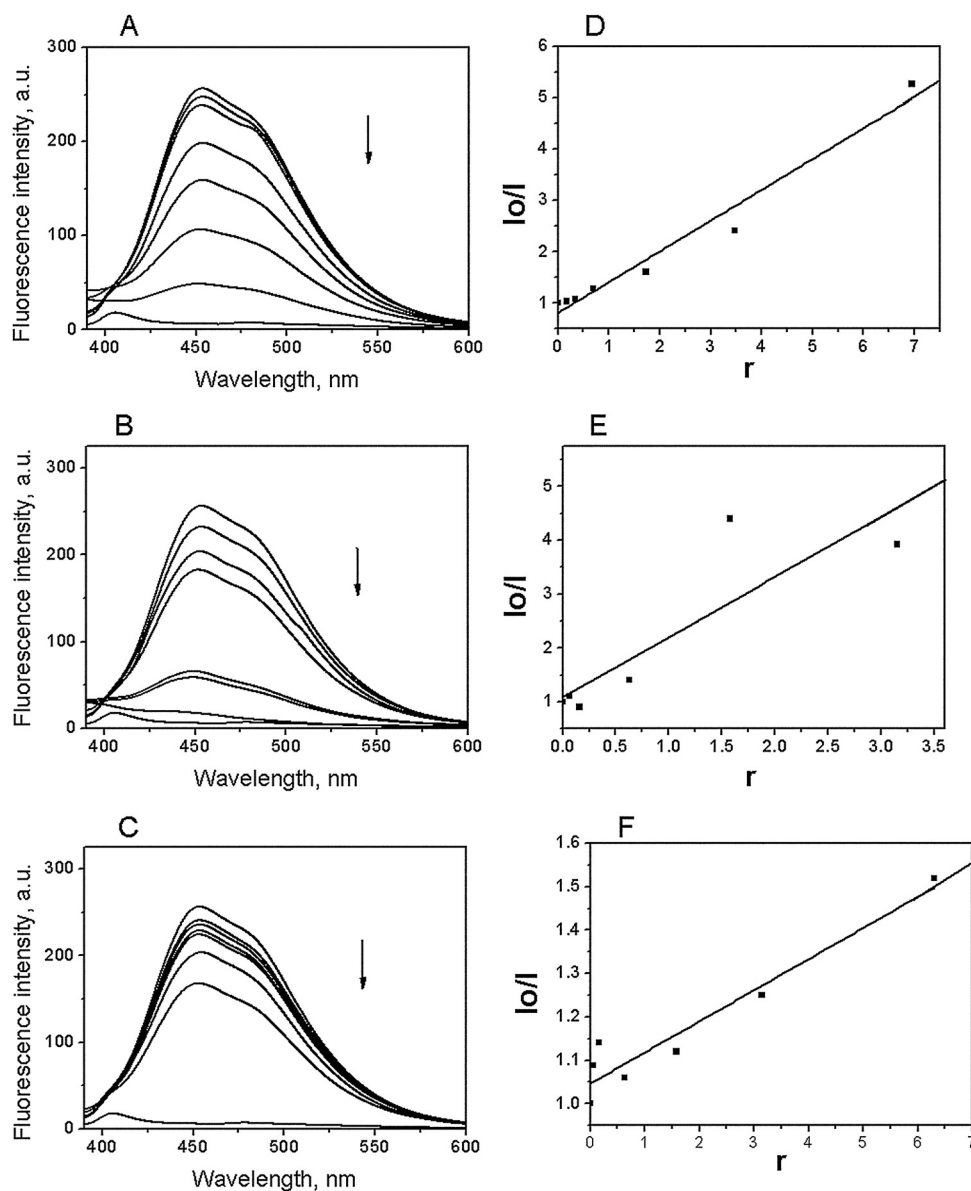


Fig. 4. Quinone interference of groove binding of Hoechst 33258 (H) with CT-DNA. Left panels: emission spectra ($\lambda_{\text{ex}} = 30 \text{ nm}$) of H alone ($25 \mu\text{M}$, bottom line), H bound to CT-DNA ($92 \mu\text{M}$, top line) and quenching of H–CT-DNA system by **2** (A), **3** (B) and **4** (C) at concentrations of 16, 32, 64, 160, 320 and $640 \mu\text{M}$, respectively (curves from top to bottom). The arrow shows that fluorescence intensity decreased with increasing concentration of the quinone. Right panels: fluorescence quenching curves of H bound to DNA at $\lambda_{\text{max}} = 453 \text{ nm}$ by **2** (D), **3** (E) and **4** (F); $r = [\text{quinone}]/[\text{CT-DNA}]$.

indicates possible degradation of DNA, which is the most extensive with 3'-(methylamino)avarone and the least extensive with its regioisomer 4'-(methylamino)avarone.

The cleaving properties of these compounds using plasmids [23,24] will be a topic of our future studies.

3.3. UV–vis spectroscopic study

The hyperchromism and hypochromism are regarded as spectral evidence for DNA double-helix structural change when DNA reacts with other molecules. The hyperchromism originates from the disruption of the DNA duplex secondary structure and the hypochromism originates from the stabilization of the DNA duplex by either the intercalation binding mode or the electrostatic effect of small molecules [25,26]. Fig. 5 shows the UV–vis absorbance spectra of **3** and **4** before and after interaction with CT-DNA.

The spectrum of **3** displayed three absorption maxima at wavelengths of 226 nm, 305 nm and 504 nm (Fig. 5A, line b). Upon its

interaction with CT-DNA, new complex **3**–CT-DNA was formed with the absorption maximum at 259 nm (Fig. 5A, line d). This blue shift in absorbance is accompanied by the hyperchromism, the value of which reached -17% (the percentage was determined from $(\epsilon_{\text{DNA}} + \epsilon_{\text{Q}}) - \epsilon_{\text{B}} / (\epsilon_{\text{DNA}} + \epsilon_{\text{Q}}) \times 100$ where ϵ_{DNA} is the extinction coefficient of CT-DNA, ϵ_{Q} is the extinction coefficient of free quinone and ϵ_{B} is the extinction coefficient of the bound quinone).

In the spectrum of **4**–CT-DNA complex (Fig. 5B, line d) the peak at 259 nm has also been observed with increase in the absorption intensity (hyperchromism was calculated as -8%).

The absorption intensity at 259 nm was increased due to the fact that purine and pyrimidine bases are exposed because of the effects of the quinone compounds, the effects of derivative **3** on the DNA molecule being more pronounced.

Different spectral features observed in the absorption spectra of **3**–CT-DNA and **4**–CT-DNA can be attributed to different regioselectivity observed in the nucleophilic addition reaction of substituted quinones. Božić et al. [27] have concluded that

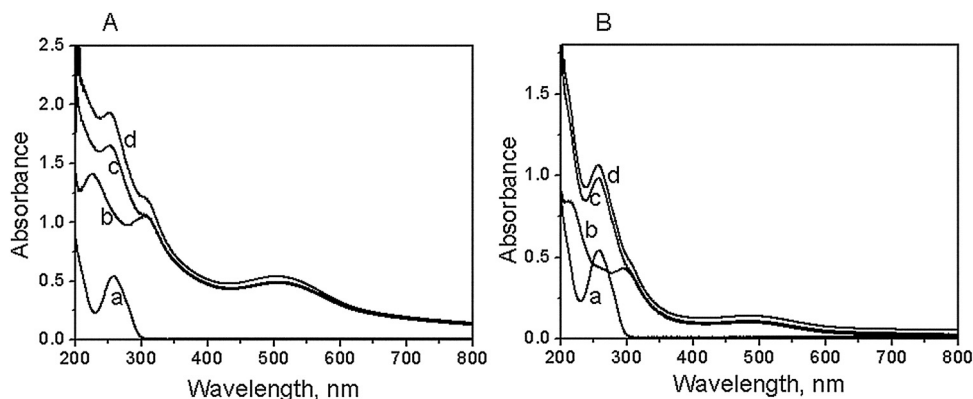


Fig. 5. Hyperchromic changes in UV–vis absorption spectra of CT-DNA (92 μ M, curve a) after interaction with 300 μ M of **3** (panel A) and **4**, (panel B). Curves b denote spectra of the quinones, curves c calculated spectra, and curves d spectra of quinone–CT-DNA.

methylamino derivative with the substituent at position 3' is a better electrophile since the more reactive 4'-position in this derivative is unsubstituted. Consequently, this derivative is much more reactive toward DNA than 4'-derivative.

The results of UV–vis spectrometry are in agreement with fluorescence investigations. As the biological effects of quinones including avarone are based in part on their ability to generate oxygen radicals [5], but also on the addition of cellular nucleophiles to the quinone moiety [28], the obtained results might also be helpful for better understanding of the mechanisms of their biological activity.

4. Conclusion

The present study reports the different electrophoretic pattern and different spectral features of the interactions of avarone, 3'-(methylamino)avarone and 4'-(methylamino)avarone with calf thymus DNA. Electrophoretic and fluorescence data revealed that quinones interfered with the intercalation of ethidium bromide. In addition, the quinones inhibited interactions of the minor groove binder Hoechst 33258 with CT-DNA. The UV–vis spectrometry supported previous results. The overall results indicated possible degradation of CT-DNA, which was the most extensive with 3'-(methylamino)avarone and the least extensive with its regioisomers 4'-(methylamino)avarone.

Acknowledgements

This work was supported by the Ministry of Education, Science and Technological Development of the Republic of Serbia (Grant 172055).

References

- [1] J.A. Mountzouris, L.H. Hurley, Small molecule–DNA interactions, in: S.M. Hecht (Ed.), *Bioorganic Chemistry: Nucleic Acids*, Oxford University Press, New York, USA, 1996, pp. 288–323.

- [2] A. Oleksi, A.G. Blanco, R. Boer, J. Uson, J. Aymami, A. Rodger, M.J. Hannon, M. Coll, *Angew. Chem. Int. Ed.* 45 (2006) 1227–1231.
- [3] R. Bera, B.K. Sahoo, K.S. Ghosh, S. Dasgupta, *Int. J. Biol. Macromol.* 42 (2008) 14–21.
- [4] Q. Saquib, A.A. Al-Khedhairi, S.A. Alarifi, S. Dutta, S. Dasgupta, J. Musarra, *Int. J. Biol. Macromol.* 47 (2010) 68–75.
- [5] C.E. Rodriguez, J.M. Fukuto, K. Taguchi, J. Froines, A.K. Cho, *Chem. Biol. Interact.* 155 (2005) 97–110.
- [6] D. Sladić, M.J. Gašić, *Molecules* 11 (2006) 1–33.
- [7] M. Vujčić, S. Tufegdžić, Z. Vujčić, M.J. Gašić, D. Sladić, *J. Serb. Chem. Soc.* 72 (2007) 1265–1269.
- [8] T. Božić, I. Novaković, M.J. Gašić, Z. Juranić, T. Stanojković, S. Tufegdžić, Z. Kljajić, D. Sladić, *Eur. J. Med. Chem.* 45 (2010) 923–929.
- [9] W.E.G. Müller, R.K. Zahn, M.J. Gašić, N. Dogović, A. Maidhof, C. Becker, B. Diehl-Seifert, E. Eich, *Comp. Biochem. Physiol.* 80 C (1985) 47–52.
- [10] L. Minale, R. Riccio, G. Sodano, *Tetrahedron Lett.* (1974) 3401–3404.
- [11] R. Cozzolino, A. De Giulio, S. De Rosa, G. Strazzullo, M.J. Gašić, D. Sladić, M. Zlatović, *J. Nat. Prod.* 53 (1990) 699–702.
- [12] M.E. Reichmann, S.A. Rice, C.A. Thomas, P. Doty, *J. Am. Chem. Soc.* 76 (1954) 3047–3053.
- [13] D. Sladić, I. Novaković, Z. Vujčić, T. Božić, N. Božić, D. Milić, B. Šolaja, M.J. Gašić, *J. Serb. Chem. Soc.* 69 (2004) 901–907.
- [14] J.R. Lakowicz, *Principles of Fluorescence Spectroscopy*, third ed., Springer, Baltimore, USA, 2006.
- [15] J.R. Lakowicz, G. Weber, *Biochemistry* 12 (1973) 4161–4170.
- [16] N.C. Garbett, N.B. Hammond, D.E. Graves, *Biophys. J.* 87 (2004) 3974–3981.
- [17] Y. Shi, C. Guo, Y. Sun, Z. Liu, F. Xu, Y. Zhang, Z. Wen, Z. Li, *Biomacromolecules* 12 (2011) 797–803.
- [18] M. Lee, A.L. Rhodes, M.D. Wyatt, S. Forrow, J.A. Hartley, *Biochemistry* 32 (1993) 4237–4245.
- [19] W.A. Prutz, *Radiat. Environ. Biophys.* 23 (1984) 1–6.
- [20] G. Zhang, X. Hu, J. Pan, *Spectrochim. Acta A* 78 (2011) 687–694.
- [21] D. Suh, J.B. Chaires, *Bioorg. Med. Chem.* 3 (1995) 723–728.
- [22] R. Kakkar, R. Garg, Suruchi, *J. Mol. Struct. (Theochem)* 584 (2002) 37–44.
- [23] M. Roy, T. Bhowmick, R. Santhanagopal, S. Ramakumar, A.R. Chakravarty, *Dalton Trans.* (2009) 4671–4682.
- [24] N. Chowdhury, S. Dutta, B. Nishitha, S. Dasgupta, N.D.P. Singh, *Bioorg. Med. Chem.* 20 (2010) 5414–5417.
- [25] X.-L. Li, Y.-J. Hu, H. Wang, B.-Q. Yu, H.-L. Yue, *Biomacromolecules* 13 (2012) 873–880.
- [26] J. Szekely, K.S. Gates, *Chem. Res. Toxicol.* 19 (2006) 117–121.
- [27] T. Božić, D. Sladić, M. Zlatović, I. Novaković, S. Trifunović, M.J. Gašić, *J. Serb. Chem. Soc.* 67 (2002) 547–551.
- [28] P.J. O'Brien, *Chem. Biol. Interact.* 80 (1991) 1–41.